Available online at www.sciencedirect.com
SCIENCE DIRECT
Journal of Magnetic Resonance 181 (2006) 233–243
JMR Journal of Magnetic Resonance
www.elsevier.com/locate/jmr

Sensitivity enhancement, assignment, and distance measurement in ^{13}C solid-state NMR spectroscopy for paramagnetic systems under fast magic angle spinning

Nalinda P. Wickramasinghe, Yoshitaka Ishii *

Department of Chemistry, University of Illinois at Chicago, Chicago IL 60607, USA

Received 28 March 2006; revised 11 May 2006
Available online 5 June 2006

Abstract

Despite success of previous studies, high-resolution solid-state NMR (SSNMR) of paramagnetic systems has been still largely unexplored because of limited sensitivity/resolution and difficulty in assignment due to large paramagnetic shifts. Recently, we demonstrated that an approach using very-fast magic angle spinning (VFMAS; spinning speed $\geqslant 20$ kHz) enhances resolution/sensitivity in ^{13}C SSNMR for paramagnetic complexes [Y. Ishii, S. Chimon, N.P. Wickramasinghe, A new approach in 1D and 2D ^{13}C high resolution solid-state NMR spectroscopy of paramagnetic organometallic complexes by very fast magic-angle spinning, J. Am. Chem. Soc. 125 (2003) 3438–3439]. In this study, we present a new strategy for sensitivity enhancement, signal assignment, and distance measurement in ^{13}C SSNMR under VFMAS for unlabeled paramagnetic complexes using recoupling-based polarization transfer. As a robust alternative of cross-polarization (CP), rapid application of recoupling-based polarization transfer under VFMAS is proposed. In the present approach, a dipolar-based analog of INEPT (dipolar INEPT) methods is used for polarization transfer and a ^{13}C signal is observed under VFMAS without ^{1}H decoupling. The resulting low duty factor permits rapid signal accumulation without probe arcing at recycle times ($\sim$3 ms/scan) matched to short ^{1}H T_1 values of small paramagnetic systems ($\sim$1 ms). Experiments on Cu(DL-Ala)$_2$ showed that the fast repetition approach under VFMAS provided sensitivity enhancement by a factor of 8–66 for a given sample, compared with the ^{13}C MAS spectrum under moderate MAS at 5 kHz. The applicability of this approach was also demonstrated for a more challenging system, Mn(acac)$_3$, for which ^{13}C and ^{1}H paramagnetic shift dispersions reach 1500 and 700 ppm, respectively. It was shown that effective-evolution-time dependence of transferred signals in dipolar INEPT permitted one to distinguish ^{13}CH, $^{13}CH_2$, $^{13}CH_3$, $^{13}CO_2^-$ groups in 1D experiments for Cu(DL-Ala)$_2$ and Cu(Gly)$_2$. Applications of this technique to 2D $^{13}C/^{1}H$ correlation NMR under VFMAS yielded reliable assignments of ^{1}H resonances as well as ^{13}C resonances for Cu(DL-Ala)$_2$ and Mn(acac)$_3$. Quantitative analysis of cross-peak intensities in 2D $^{13}C/^{1}H$ correlation NMR spectra of Cu(DL-Ala)$_2$ provided distance information between non-bonded ^{13}C–^{1}H pairs in the paramagnetic system.

Keywords: ^{13}C solid-state NMR; Paramagnetic systems; Fast MAS; Sensitivity; Assignments; Distances

1. Introduction

Metals whose ions exhibit paramagnetism occupy more than one-third of the periodic table. In nature, diverse paramagnetic metal ions are utilized as catalytic centers in complexes with organic ligands [1]. Paramagnetic organometallics or metal coordination complexes in solids have attracted increasing interest in conjunction with supramolecular chemistry [2,3], medicinal chemistry [4–6], and solid-state synthesis [7].

High-resolution solid-state NMR (SSNMR) spectroscopy has been widely used for structural analysis of non-crystalline compounds in solids [8–10]. In particular, ^{13}C high-resolution SSNMR has been one of the most powerful techniques for analysis of organic materials including polymers and biomolecules, for which single crystals are often

* Corresponding author. Fax: +1 312 996 0431.
E-mail address: yishii@uic.edu (Y. Ishii).

1090-7807/$ - see front matter © 2006 Elsevier Inc. All rights reserved.
doi:10.1016/j.jmr.2006.05.008

not available [10–21]. Assisted by recent methodological development for quadrupolar nuclei [22–26], ^{13}C SSNMR has also provided metal binding structures in analysis of diamagnetic metal complexes [27–29]. ^{13}C SSNMR is a potentially powerful method for characterizing paramagnetic organic systems without the requirement of isotope-labeled materials. In contrast, for paramagnetic organic complexes, applications of ^{13}C SSNMR and SSNMR of other dilute spin-1/2 nuclei have been notably limited, despite the success of previous studies [30–38].

^{13}C paramagnetic shift dispersions can range from several hundreds to a few thousands of ppm, while those in ^{1}H SSNMR can vary from several tens to several hundreds of ppm [34,38,39]. Because of the large paramagnetic shifts, fundamental methods in ^{13}C SSNMR such as CP, MAS, and RF decoupling have been generally ineffective for paramagnetic systems. The large anisotropies of paramagnetic shifts split a signal into many sidebands, limiting resolution and sensitivity enhancement by MAS [39]. Because of the sensitivity limitation, a MAS probe that can accommodate a relatively large sample volume ($\geqslant$100 μL) has been traditionally utilized, in particular, for unlabeled paramagnetic samples. Moderate ^{1}H RF decoupling fields in this type of SSNMR probe barely cover the spectral range of many paramagnetic systems, severely limiting the resolution and sensitivity [33]. Liu et al. [34] reported line narrowing of ^{13}C MAS spectra for unlabeled systems without decoupling under a moderate spinning speed of ~10 kHz. In spite of the excellent result, the moderate spinning speed is useful only for systems having a small ^{1}H–^{1}H dipolar flip-flop rate due to a large ^{1}H shift dispersion, isotopic dilution, or molecular motions [34,38,40]. For this reason, ^{2}D-labeled paramagnetic compounds have been generally utilized in ^{13}C SSNMR to remove ^{1}H–^{13}C couplings without ^{1}H RF decoupling [33,34,37,41]. Furthermore, polarization transfer by CP, a vital technique in ^{13}C SSNMR , has been ineffective for many paramagnetic systems because of the large shift dispersions, except in a few successful cases for compounds having small shift dispersions [30,36,37].

Equally critical elements in ^{13}C SSNMR analysis of paramagnetic compounds are signal assignments. Large paramagnetic shifts mask diamagnetic shifts specific to chemical groups, making signal assignments difficult. Recoupling techniques and multi-dimensional NMR have been widely used in signal assignments for diamagnetic systems [11,43]. However, recoupling techniques have not been applied to paramagnetic systems because of the limited sensitivity and the lack of effective decoupling methods. Only a few 2D SSNMR experiments have been performed for ^{13}C-labeled small paramagnetic systems [35,37]. Thus, even if ^{13}C SSNMR spectra can be obtained for unlabeled systems, reliable signal assignments have required selectively ^{13}C- and/or ^{2}D-labeled samples [34,39]. To advance SSNMR analysis of paramagnetic systems, we recently presented a new approach to obtain high-resolution ^{13}C and ^{1}H SSNMR of paramagnetic complexes using very-fast MAS (VFMAS) at a spinning speed (ν_R) of 20 kHz or higher [42,44]. In this approach, sensitivity and resolution in ^{13}C and ^{1}H SSNMR of paramagnetic systems are enhanced by VFMAS, which effectively removes ^{1}H–^{13}C and ^{1}H–^{1}H dipolar couplings without RF irradiation. Although MAS at 40 kHz or more is currently available [45], this spin dynamics, which forms the foundation of our approach, is not altered qualitatively by faster spinning ($\nu_R > 30$ kHz).

In this article, we examine the effectiveness of the VFMAS approach for characterization and structural elucidation of unlabeled paramagnetic systems by ^{13}C SSNMR. Although this study is focused on ^{13}C SSNMR, the presented strategy can be applied to other spin-1/2 systems in paramagnetic systems. We demonstrate that reliable signal assignment and structural information can be obtained with enhanced sensitivity and resolution by combination of VFMAS and dipolar recoupling techniques. We show that sensitivity of ^{13}C SSNMR of paramagnetic systems obtained by a fast repetition of a recoupling-based polarization-transfer sequence can be comparable to or higher than that of corresponding diamagnetic molecules. It is also shown that 2D $^{13}C/^{1}H$ correlation NMR is possible for paramagnetic system with large spectral dispersion by use of the recoupling-based polarization transfer for assignments and structural measurements.

2. Materials and methods

2.1. Sample preparation

Cu(II)(DL-alanine)$_2 \cdot (H_2O)$ (Cu(DL-Ala)$_2$) was prepared following Ref. [34]. All the materials required for the synthesis were purchased from Sigma–Aldrich Co. (St. Louis, MO). Mn(III)(acac)$_3$, Cu(II)(glycine)$_2$ (Cu(Gly)$_2$), and L-Ala used for the measurement were also purchased from Sigma–Aldrich Co.

2.2. Solid-state NMR spectroscopy

All the SSNMR spectra were acquired at 9.4 T (400 and 100 MHz for ^{1}H and ^{13}C NMR, respectively) with a Varian Infinityplus 400 NMR spectrometer (Palo Alto, CA) using a Varian 3.2-mm MAS double-resonance T3 NMR probe and a home-built 2.5-mm MAS double-resonance probe. The 3.2- and 2.5-mm MAS probes provide stable spinning up to 24 and 29 kHz, respectively. Fluctuation of the spinning speed was less than 10 Hz throughout the experiments. All the data were processed with Varian Spinsight software or NMRPipe software [47].

For the single π/2-pulse excitation experiments in ^{13}C SSNMR, a rotor-synchronous echo sequence (τ_R–π–τ_R) was applied prior to signal acquisition, where τ_R denotes a MAS rotation period. In this sequence, a signal was excited by a π/2-pulse and then acquired after two rotation periods, at the middle of which a π-pulse was applied in order to refocus large isotropic chemical shifts in paramagnetic complexes. For ^{13}C NMR by single π/2-pulse

excitation, recycle times of the single pulse excitation experiments were set to three times the ^{13}C T_1 values or M_{dec} times a ^1H RF decoupling period, whichever is longer, where $M_{dec} = 100$ and 75 for the 3.2- and 2.5-mm MAS probes, respectively. The value M_{dec} was selected for protecting the probes from arcing. For polarization transfer with CP, an adiabatic CP sequence [48,49] was used to compensate for variation of Hartmann–Hahn conditions for large resonance offsets in paramagnetic systems [42]. In the CP experiments, the recycle time was set to M_{dec} times the contact time. A rotor-synchronous echo sequence was also used in the CP experiment before signal acquisition. In ^{13}C dipolar INEPT experiments [46,50], a modified dipolar INEPT sequence was used for polarization transfer without ^1H RF decoupling, as will be described in the text. The recycle time for the dipolar INEPT experiments was adjusted to three times the ^1H T_1 values. In all the experiments, the π-pulse widths were twice the π/2-pulse widths unless otherwise mentioned.

Because paramagnetic isotropic shifts have a $1/T$ dependence (Curie's law) in the high-temperature approximation [51], both spinning speed and RF-duty factor were found to affect observed chemical shifts. For experimental simplicity, we indicated the temperature of VT cooling air rather than that of a sample. Unless otherwise mentioned, cooling air at room temperature (23 °C) was used. The flow rate of the cooling air, which also affects the temperature difference, was set to 140–160 $(ft)^3/h$. The relatively high flow rate helps to minimize line broadening due to temperature distribution over a sample. The temperature difference between a sample and the cooling air, ΔT, was calibrated by ^{207}Pb shift using $PbNO_3$ [52]. The temperature difference between a sample and the cooling air ΔT (°C) approximately followed the relationship $\Delta T = 0.0607\nu_R^2$ and $\Delta T = 0.0600\nu_R^2$ for 3.2- and 2.5-mm probes, respectively, where ν_R is in units of kHz. Because of the short recycle delays required in some of our experiments, care was taken so that no hidden delays were included between scans. For example, when the recycle time was comparable to the acquisition time, the acquisition period was included as a part of the recycle time.

Simulations for dipolar INEPT experiments were performed by numerically integrating a Liouville–von Neuman equation with Hamiltonian under a relevant pulse sequence using a home-built Fortran program. The time dependence of the NMR signal was obtained by calculating the observable for different crystalline orientations in a time step of 0.25 μs. The powder average of a simulated signal was performed over 15,500 orientations in (10°, 10°, 15°) angular steps for the Euler angles (α, β, γ).

3. Results and discussion

3.1. Sensitivity enhancement by VFMAS and polarization transfer

Fig. 1 demonstrates the sensitivity enhancement in ^{13}C SSNMR spectrum by VFMAS for a paramagnetic system. Fig. 1a–d shows spinning-speed dependence of ^{13}C MAS spectra of Cu(DL-Ala)$_2$, which was obtained at ν_R = (a) 5, (b) 10, (c) 15, and (d) 24 kHz. Each spectrum in (a–d) was acquired with the same number of scans in a common total

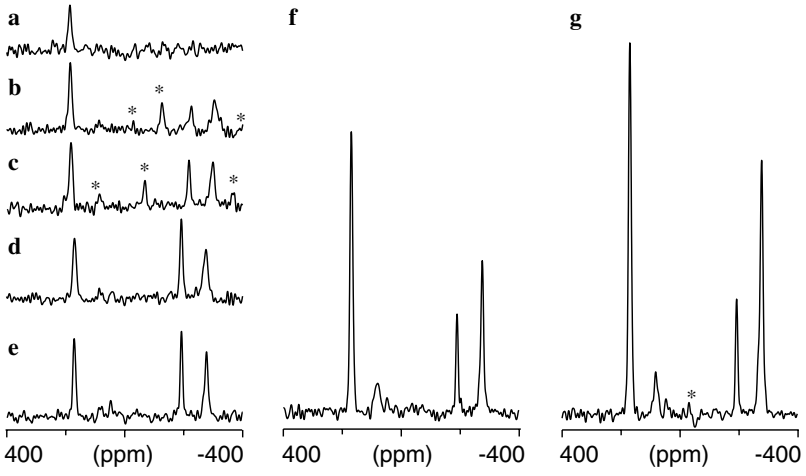

Fig. 1. ^{13}C MAS spectra of Cu(DL-alanine)$_2 \cdot (H_2O)$ obtained at a ^{13}C NMR frequency of 100.6 MHz with (a–e) a single π/2-pulse excitation, (f) adiabatic-CP, and (g) dipolar INEPT. The spectra were acquired at spinning speed of (a) 5 kHz, (b) 10 kHz, (c) 15 kHz, and (d–g) 24 kHz. The spectra (a–d) were obtained under ^1H cw RF decoupling (100 kHz) irradiated at 15.3 ppm, while the spectra (e–g) were acquired without ^1H RF decoupling. The recycle delays of 0.1 s in (a–e) and 4.5 ms in (g) were matched to three times the ^{13}C and ^1H T_1 values, respectively. The recycle time in (f) (0.05 s) was restricted by an RF-duty factor (1%) to prevent a probe arcing. For each spectrum, signals were accumulated during an acquisition time of 1.0 ms with a total experimental time of 1 min with (a–e) 614, (f) 1,200, and (g) 13,556 scans. In (g), the dipolar INEPT pulse sequence shown in Fig. 2a was used with $\tau = 27$ μs. The spectra are scaled by a factor of $1/N^{1/2}$, where N is the number of scans, so that all display a common noise level for comparison. The ^{13}C and ^1H π/2-pulse widths were 2.5 μs. In the CP experiment, the ^{13}C RF field was swept from 107.5 to 124.5 kHz during a contact time of 0.5 ms, while the ^1H RF field was kept constant at 92 kHz. For each spectrum, a Gaussian broadening of 300 Hz was applied. The spinning sidebands are indicated by *. The peak at ~100 ppm is attributed to impurity or minor species. The sample amount was 15 mg.

experimental time of 1 min under ^{1}H decoupling of 100 kHz. In Fig. 1a at $\nu_R = 5$ kHz, only one signal that was assigned to the CH_3 group is visible around 200 ppm, reflecting the fact that this chemical group has a relatively small paramagnetic anisotropic shift. Signals for CO_2^- and CH are within the noise level because of the signal splitting into many sidebands and line broadening. Fig. 1b–d clearly shows the improvement in resolution under faster MAS by reduction of sideband intensities. Under VFMAS at 24 kHz in (d), three lines assigned to CH_3, CO_2^-, and CH signals display good sensitivity and resolution at 172, −192, and −277 ppm, respectively. Although considerable number of sidebands due to anisotropic paramagnetic shifts are visible in (b, c), sidebands were almost completely suppressed in (d). The anisotropic paramagnetic interactions originating mainly from pseudocontact shifts [40,53] have the same form as a usual anisotropic shift and can be removed by MAS [54]. Fig. 1e shows a ^{13}C MAS spectra obtained at 24 kHz without ^{1}H RF decoupling. Resolution and sensitivity in (e) are superior to those in (d) obtained with ^{1}H RF decoupling, particularly for the CH signal at −277 ppm. This result demonstrates that ^{1}H–^{13}C dipolar couplings can be more effectively removed by VFMAS than by strong ^{1}H RF irradiation at 100 kHz for paramagnetic complexes having a relatively large ^{1}H spectral dispersion due to isotropic and anisotropic paramagnetic shifts (∼200 ppm). This is reasonable because averaging of ^{1}H–^{13}C dipolar coupling by VFMAS functions regardless of ^{1}H resonant offset. Hence, despite a common belief that ^{13}C SSNMR requires high-power ^{1}H RF decoupling, ^{1}H RF decoupling can be safely dropped under VFMAS for paramagnetic compounds. Although linewidths are still broader than those for diamagnetic systems, excellent resolution was obtained because the lines are well separated by large isotropic paramagnetic shifts originating from Fermi contact shifts [40,53].

Further sensitivity enhancement of ^{13}C SSNMR of a paramagnetic system is possible with polarization transfer from ^{1}H spins. In our previous work [42], it was demonstrated that a ramped high-power CP is applicable to paramagnetic systems. However, in CP experiments, recycle times are restricted by RF-duty factors to prevent probe arcing rather than by ^{1}H T_1 values because of a relatively long contact period in CP (∼ms). If the RF-duty factor can be reduced, faster repetitions with recycle times matched to short ^{1}H T_1 values (∼1 ms) in small paramagnetic systems are possible for sensitivity enhancement. Based on this idea, we propose here a simple yet effective strategy, rapid application of recoupling-based polarization transfer using a dipolar INEPT sequence. The dipolar INEPT sequence was originally developed by Vita and Frydman [46] for organic compounds under moderately fast MAS (10–14 kHz). An equivalent method was discussed as recoupled polarization transfer (REPT) by Saalwachter et al. [50]. Although this sequence does not provide a sensitivity advantage over CP for diamagnetic systems, its much smaller duty factor than CP is optimal in our experiments for paramagnetic systems. Fig. 2a shows our dipolar INEPT/REPT pulse sequence modified for paramagnetic systems. As will be discussed in a later section, the effective evolution period under recoupled ^{1}H–^{13}C dipolar couplings can be adjusted by varying the τ period in Fig. 2a [46]. It is noteworthy that the original sequence in Ref. [46] reintroduces large ^{1}H paramagnetic anisotropic shifts, and thus is not suitable for paramagnetic systems. On the other hand, this sequence in Fig. 2a properly transfers polarization, eliminating large ^{1}H and ^{13}C anisotropic shifts and ^{1}H–^{1}H dipolar couplings under VFMAS. Fig. 1g shows a ^{13}C VFMAS spectrum obtained with the dipolar INEPT sequence at $\nu_R = 24$ kHz in the same experimental time (1 min) as that for (a–d). Clearly, Fig. 1g shows unexpectedly high sensitivity; the sensitivity enhancements in Fig. 1g are 4.0–4.9, and 1.4 compared with the VFMAS spectrum in Fig. 1e for protonated and non-protonated ^{13}C signals, respectively.

Below, we discuss the high sensitivity in Fig. 1g in order to ascertain the general applicability of our approach under VFMAS with dipolar INEPT. Because of short ^{1}H T_1 values (1–1.5 ms), which are much shorter than ^{13}C T_1 values (10–33 ms) and the resultant extremely short experimental recycle times of 4.5 ms in Fig. 1g, the number of scans (13,556 scans) was significantly increased within the given experimental time. We set τ to 27 μs ($0.66\tau_R$) to optimize polarization-transfer efficiency to $^{13}CH_3$, while obtaining about 80% of the maximum polarization transfer to CH and CO_2^-. In Fig. 1f using high-power ramped CP with recycle delays of 50 ms, the corresponding enhancement factors for the same sample are 2.2−3.6 and 1.2, respectively. Hence, sensitivity enhancement by rapid application of dipolar INEPT is considerably higher than that by ramped CP. More importantly, the dipolar INEPT-VFMAS approach does not require adjustments of the Hartmann–Hahn condition, which are often challenging in CP-VFMAS experiments for unlabeled paramagnetic samples. Compared with the conventional MAS spectrum obtained at 5 kHz in Fig. 1a, significant sensitivity enhancement is apparent in Fig. 1g; from the spectra, we estimate sensitivity enhancement factors of 66, 11, and 8 for CH, CO_2^-, and CH_3, respectively. It is noteworthy that the excellent signal-to-noise (S/N) ratios (67 for CH_3, 19 for CO_2^-, 42 for CH) in (g) were obtained in 1 min for only 15 mg of a non-labeled sample. In fact, another control experiment showed that the S/N ratios obtained for the equimolar amount (11.2 mg) of L-Ala are 58, 49, and 35 for CH_3, CO_2^-, and CH, respectively, where the spectrum for L-Ala was obtained at $\nu_R = 24$ kHz by a ramped CP with ^{1}H TPPM decoupling (100 kHz) for 1 min (20 scans) using a matched window function (Gaussian 30 Hz). Thus, as a result of the fast repetition strategy, for Cu(DL-Ala)$_2$, we could attain sensitivity comparable to or slightly higher than the equimolar diamagnetic system.

To further test the generality of the VFMAS approach for systems possessing extremely large paramagnetic shifts, we chose Mn(acac)$_3$ (acac = CH_3–CO–CH–CO–CH_3) as a test

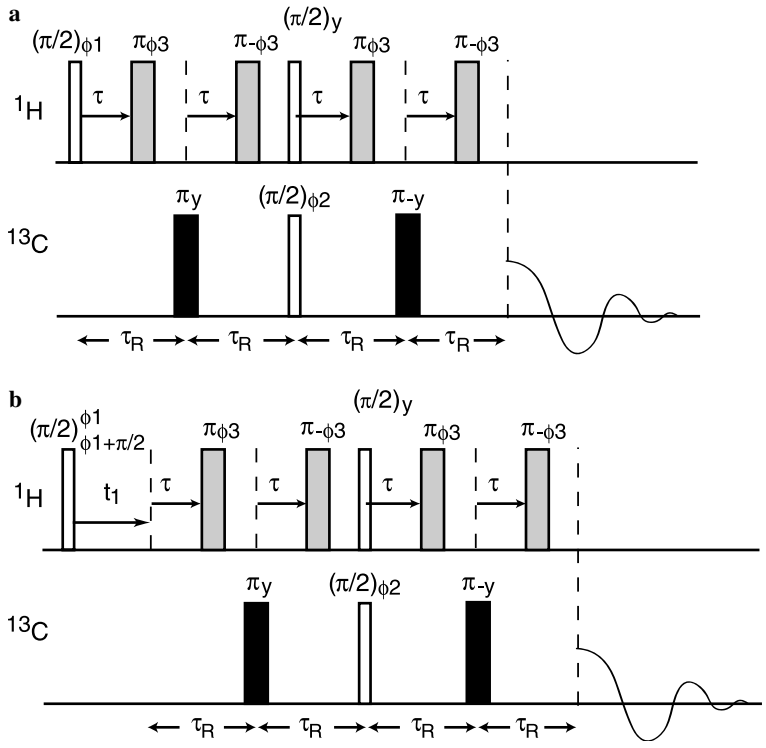

Fig. 2. Pulse sequences of (a) 1D ^{13}C dipolar INEPT for paramagnetic systems and (b) 2D ^{13}C/^{1}H chemical-shift correlation NMR with the dipolar INEPT polarization transfer. In (a), after ^{1}H transverse magnetization was transferred by a $\pi/2$-pulse, a rotor-synchronous echo sequence applied to ^{1}H and ^{13}C spins during the initial two rotor cycles ($2\tau_R$) reintroduces ^{1}H–^{13}C dipolar interaction while canceling ^{1}H anisotropic shifts. Simultaneous applications of $\pi/2$-pulses to ^{1}H and ^{13}C spins convert antiphase transverse magnetization of ^{1}H spins to that of ^{13}C spins. After the polarization transfer is completed by the second echo sequence, ^{13}C signal is detected. The phase cycles are as follows: $\phi_1 = x, -x$; $\phi_2 = -y, -y, y, y$; $\phi_3 = y, y, y, y, -y, -y, -y, -y$; the receiver phase $= x, x, -x, -x$. In (b), the t_1 period for ^{1}H isotropic shift evolution was inserted between the initial $\pi/2$-pulse to ^{1}H spins and the dipolar INEPT period. The real or imaginary component of the ^{1}H signal is selectively transferred to ^{13}C spins by applying the initial $\pi/2$-pulse to ^{1}H spins along x or y axis in the rotating frame, respectively. The phase cycles are the same as those for (a).

case. Because the electron spin state, S, is 2 for Mn(III) and anisotropic paramagnetic shifts due to pseudocontact shifts are proportional to $S(S+1)$ [40], this sample displays significantly larger ^{13}C and ^{1}H anisotropic shifts than those of Cu(DL-Ala)$_2$ ($S = 1/2$). The range of the ^{13}C paramagnetic shift dispersion is about 1500 ppm for this system. A previous study by Liu et al. reported that ^{13}C signals were undetectable under MAS at 11 kHz [34]. A recent high-frequency EPR study showed that EPR analysis of the polycrystalline Mn(acac)$_3$ was difficult [55]. In Fig. 3, we demonstrate that even for systems having large shift dispersions, the VFMAS approach can provide significantly improved resolution and sensitivity. Fig. 3a–d shows spinning-speed dependence of the ^{13}C VFMAS spectrum of Mn(acac)$_3$ under ^{1}H RF decoupling of 100 kHz. For the present sample, the effect of VFMAS appears less dramatic with ^{1}H decoupling. The signals, which are unresolved at (a) 5, (b) 10 kHz, exhibit limited resolution even at (d) 26.3 kHz.

We found that sensitivity/resolution can be greatly enhanced by dropping ^{1}H decoupling, as shown in Fig. 3e. ^{1}H anisotropic shifts for this sample reach 700 ppm (~300 kHz for ^{1}H NMR freq. of 400 MHz) [44], and hence ^{1}H RF decoupling is ineffective even with high-power ^{1}H RF decoupling at 100 kHz. In contrast, ^{1}H–^{13}C dipolar averaging by VFMAS is effective regardless of ^{1}H resonance offsets, and thus ^{1}H decoupling by VFMAS provides improved resolution and sensitivity in ^{13}C NMR spectra even for the complex having an extremely large ^{1}H paramagnetic shift dispersion. Dropping ^{1}H decoupling also enabled us to triple the repetition rate of the signal acquisition (~66 scans/s), which was limited by ^{1}H RF-duty factors in (a–d) rather than ^{13}C T_1 values. All the spectra in Fig. 3 were obtained with a common experimental time (10 min) and display a common noise level for comparison. As shown in Fig. 3, the sensitivity enhancement in (e) was 4–7 times compared with the conventional MAS spectrum in (b). Since signals in Fig. 3e are well resolved, it is possible to estimate the range of anisotropic paramagnetic shifts from spinning sideband analysis, which permits measurement of the metal–^{13}C distance, as will be discussed elsewhere [56].

We also examined the possibility of sensitivity enhancement by polarization transfer under VFMAS for a sample possessing extremely large paramagnetic shifts, again using Mn(acac)$_3$. Fig. 3f shows a 1D ^{13}C VFMAS spectrum of Mn(acac)$_3$ obtained by rapid application of dipolar INEPT (1.5 ms/scan) in a common experimental time with (a–e) (10 min). The spectrum was obtained by setting $\tau = 9$ μs ($0.237\ \tau_R$) to optimize the polarization-transfer efficiency for ^{13}CH and ^{13}CH$_3$ in the dipolar INEPT sequence (see

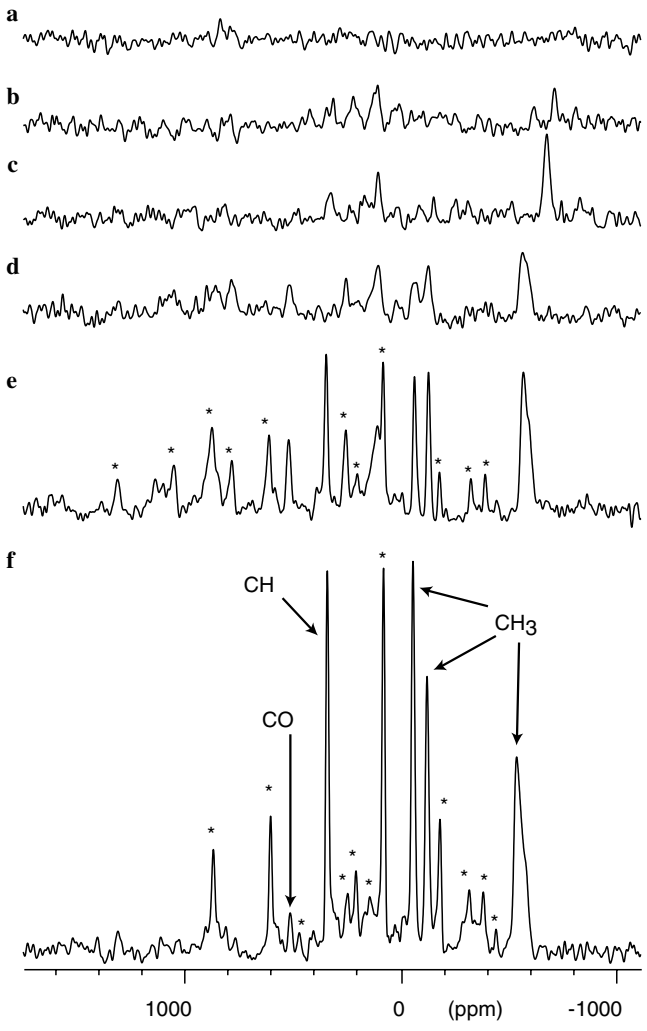

Fig. 3. ^{13}C MAS spectra of $Mn(acac)_3$ obtained at ^{13}C NMR frequency of 100.6 MHz with (a–e) a single $\pi/2$-pulse excitation and (f) the dipolar INEPT sequence shown in Fig. 2a. The spectra were acquired at spinning speed of (a) 5, (b) 10, (c) 16, and (d–f) 26.3 kHz. While the spectra in (a–d) were obtained under ^{1}H cw decoupling (100 kHz) irradiated at 15 ppm with recycle delays (τ_d) of 45 ms, those in (e) and (f) were acquired under VFMAS without ^{1}H RF decoupling with τ_d of 15 and 1.5 ms, respectively. The ^{13}C and ^{1}H $\pi/2$-pulse widths were 1.7 μs. All the spectra were acquired at −15 °C in a common experimental time of 10 min with (a–d) 13,110, (e) 39,940, and (f) 364,540 scans. As in Fig. 1, the spectra are scaled to exhibit a common noise level for comparison. Gaussian broadening of 1,200 Hz was applied. The spinning sidebands are indicated by * only for (e, f). The assignments in (f) are based on a separate ^{13}C–^{1}H REDOR experiment (see Table 1 in the later section).

the next section about the details). With the shortened recycle times reflecting short ^{1}H T_1 values (~0.5 ms), the number of scans was substantially increased for a given experimental time. With a short τ value in the dipolar INEPT sequence, the resulting spectrum displays strong signals only for protonated ^{13}C because of the short effective transfer period. It is clear that a relatively complicated spectrum in Fig. 3e is simplified in (f) because of the semi-selective enhancement for protonated ^{13}C signals. The signal assignment in Fig. 3f was obtained by a separate ^{13}C–^{1}H REDOR experiment, as will be discussed in the later section [42]. The sensitivity enhancements by our approach for protonated ^{13}C are estimated to be factors of up to 2.8 and 20, compared with the VFMAS spectrum in (e) ($\nu_R = 26.3$ kHz) and the MAS spectrum in (b) ($\nu_R = 10$ kHz), respectively. Since there had been no means to transfer polarization effectively for this class of paramagnetic compounds having spectral dispersion over 1500 ppm, the techniques developed here can be utilized as an essential building block to correlate ^{13}C and ^{1}H spins in more advanced experiments. Although sensitivity enhancement for non-protonated ^{13}C was not achieved for this complex, this may be possible by future improvements of polarization-transfer sequences. In a control experiment, we found that CP leads to no sensitivity enhancement. Although it was possible to increase signal intensities by CP for each scan, the large duty factor of the CP sequence limited its repetition rate to a much lower value than that for the direct excitation by a ^{13}C single $\pi/2$-pulse; as a result, no sensitivity enhancement was achieved with CP for this sample having short ^{13}C T_1 values (~5 ms). It is also worth mentioning that because of a short polarization transfer time (4 τ_R) our approach is also effective for samples having short $T_{1\rho}$, for which CP is not useful.

3.2. Signal assignments in 1D ^{13}C NMR

Even if well-resolved signals are observed, signal assignment often remains a major challenge in analysis of SSNMR spectra of paramagnetic systems. Large paramagnetic shifts mask diamagnetic shifts specific to chemical groups, making spectral assignments problematic. We recently proposed *signal editing* [16,57,58] for paramagnetic systems, based on ^{1}H–^{13}C dipolar recoupling techniques, in which dipolar couplings are reintroduced by RF pulses under MAS in a controlled manner [42]. In spite of the growing importance of recoupling techniques, these methods have not been applied to ^{13}C and ^{1}H NMR of paramagnetic complexes because the large paramagnetic shifts hinder ^{1}H and ^{1}H–^{1}H RF decoupling, which are generally required in recoupling. As already shown, our VFMAS approach resolves the decoupling problems. However, in our previous signal editing method using ^{1}H–^{13}C REDOR, distinction between CH and CH_2 signals has been difficult [42]. Also, quantitative analysis of signal intensities was difficult when sensitivity enhancement by CP was employed for paramagnetic systems.

As an alternative approach for assignments and quantitative analysis, we propose signal editing by a dipolar INEPT method under VFMAS [46,50]. Frydman et al. recently showed that this method permits distinction of CH, CH_2, and CH_3/–C– groups under moderately fast MAS (10–14 kHz), where –C– denotes non-protonated carbon. However, the effectiveness of this method at a faster MAS condition and applicability of this technique to paramagnetic systems with larger spectral dispersion have not been examined. Fig. 4a–d shows the experimental results

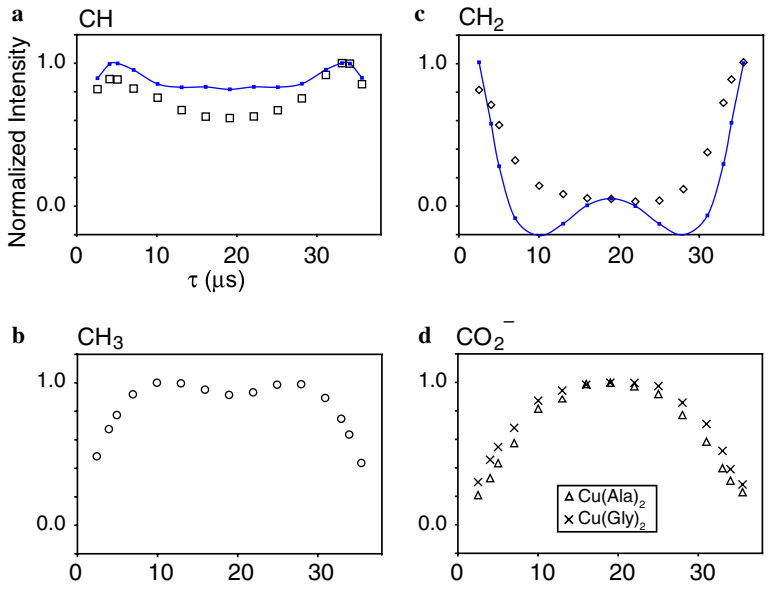

Fig. 4. Experimental τ-dependence (black markers) of signal intensities in dipolar INEPT experiment of ^{13}CH (a) and $^{13}CH_3$ (b) in Cu(DL-alanine)$_2$, $^{13}CH_2$ (c) in Cu(glycine)$_2$, and $^{13}CO_2^-$ (d) for the both samples, together with simulated data for CH and CH_2 plotted by blue markers with solid lines for eye guides. The signal intensities were normalized by the maximum intensity in each plot. The pulse sequence in Fig. 2a was used. The spinning speed was set to 23.81 kHz ($\tau_R = 42$ μs). For both ^1H and ^{13}C spins, $\pi/2$- and π-pulse widths were 2 and 4 μs, respectively. (For interpretation of the references to color in this figure legend, the reader is referred to the web version of this paper.)

for paramagnetic systems: τ-dependence of (a) CH and (b) CH_3 signals in Cu(DL-Ala)$_2$, (c) CH_2 signal in Cu(Gly)$_2$ and (d) CO_2^- signals in Cu(DL-Ala)$_2$ and Cu(Gly)$_2$ with simulated curves for ^{13}CH and $^{13}CH_2$. The experimental curves in Fig. 4 reasonably agree with the simulated ones for CH and CH_2, where C–H distances of 1.10 Å and a H–C–H angle of 108.4° for the simulation were adopted from the X-ray structure [59]. The slow build-up curves for the CO_2^- groups are as expected since this ^{13}C has no directly attached ^1H. In the original dipolar INEPT sequence under moderately fast MAS [46], distinction between $^{13}CH_3$ and non-protonated ^{13}C was difficult. In the present experiment, the experimental oscillation patterns display clear difference between CH_3 and CO_2^- groups. We also confirmed that the obtained τ-dependence curves agree well with those in control experiments for diamagnetic systems (CH, CH_2, CH_3, CO_2^-), L-Ala and Gly (data not shown).

We demonstrated τ-dependence of signal intensities provide reliable signal assignment. However, it may not be practical to obtain several data points for different τ periods for samples with limited sensitivity. In such a case, it is possible to distinguish CH, CH_2, CH_3, and –C– by simply comparing the ratio of signal intensities for two different τ values. For example, in Fig. 4, the ratios of the experimental signal intensities between $\tau = 4$ μs and 19 μs, [I(19 μs)/I(4 μs)], are 69, 6, 136, and 217–303% for CH, CH_2, CH_3, and CO_2^- groups, respectively. In control experiments on L-Ala and Gly, we obtained consistent values, [I(19 μs)/I(4 μs)], of 68, 3, 128, and 252–282% for CH, CH_2, CH_3, and CO_2^-, respectively. This clear dependence of the ratios on spin topologies provides an efficient method for signal assignments. These results show that the CH, CH_2, CH_3, and C signals can be easily distinguishable by a few dipolar INEPT experiments under VFMAS for small quantities of non-labeled paramagnetic systems (~15 mg).

3.3. Signal assignments in 2D $^{13}C/^1H$ heteronuclear correlation NMR

2D $^{13}C/^1H$ correlation NMR has been widely used as a technique to obtain signal assignment and information on molecular structure and dynamics for organic molecules including synthetic materials, polymers, and biomolecules [8,10,60–63]. However, for paramagnetic systems, this powerful technique has not been utilized due to lack of effective polarization-transfer techniques, difficulty of ^1H–^1H decoupling, and limited sensitivity. We recently demonstrated that by combination of high-power ramped CP and VFMAS, 2D $^{13}C/^1H$ correlation NMR is possible for paramagnetic complexes [42]. In this method, ^1H–^1H dipolar coupling is simply removed by VFMAS [42,44]. However, with CP transfer, quantitative interpretation of signal intensities has been difficult. Also, resonance offset dependence of CP transfer efficiency has limited application of this 2D $^{13}C/^1H$ correlation technique to paramagnetic systems of large ^{13}C shift dispersion. Here, we demonstrate that 2D $^{13}C/^1H$ correlation NMR with dipolar INEPT transfer addresses these problems, providing a novel way to obtain signal assignment and structural information.

Fig. 5a shows a 2D $^{13}C/^1H$ correlation NMR spectrum of Cu(DL-Ala)$_2$ obtained with dipolar INEPT transfer with

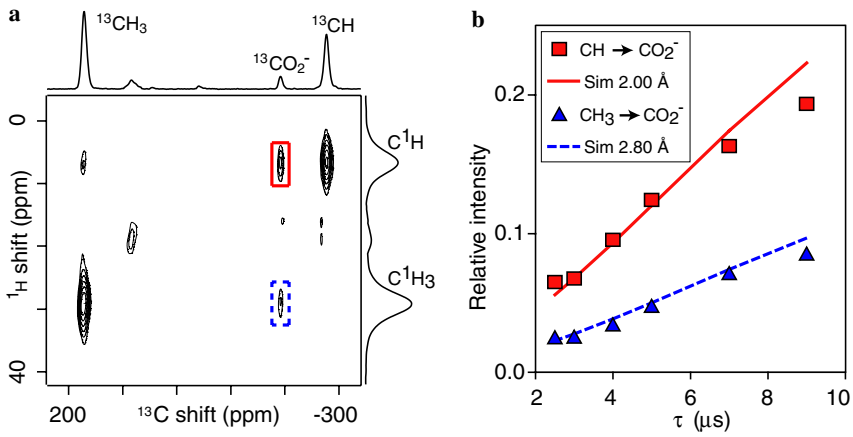

Fig. 5. (a) 2D $^{13}C/^1H$ correlation NMR spectrum of Cu(DL-Ala)$_2 \cdot H_2O$ obtained with the pulse sequence using dipolar INEPT transfer shown in Fig. 2b at $\tau = 9$ μs. The experiment was performed at spinning speed of 23,810 ± 10 Hz at 24 °C for 15 mg of the sample. Twenty t_1 complex points were recorded with a t_1 increment of 42.0 μs (τ_R) and 768 scans for the real and imaginary components of each t_1 point. The recycle time was 5.5 ms including a signal acquisition period (1.5 ms) for each scan, and the total experimental time was 3.1 h. For both of ^1H and ^{13}C spins, π/2- and π-pulse widths were 2 and 4 μs, respectively. Gaussian broadening of 300 Hz was applied in the t_1 and t_2 periods. (b) τ-Dependence of signal intensities in 2D $^{13}C/^1H$ correlation experiments for the cross-peak between C^1H and $^{13}CO_2^-$ (■) and that between C^1H_3 and $^{13}CO_2^-$ (▲) signals for Cu(DL-alanine)$_2$, together with best-fit simulated curves for ^{13}C–^1H distances of 2.0 Å (—) and 2.8 Å (····). The data in (b) were obtained in the same condition as in (a) except for τ. The signal intensities were normalized by the maximum intensity for the cross-peak within the CH group. (For interpretation of the references to color in this figure legend and text citation, the reader is referred to the web version of this paper.)

$\tau = 9$ μs. The pulse sequence in Fig. 2b was used for this experiment. For directly bonded ^{13}C–^1H pairs, we obtained cross-peaks at $(\omega_H, \omega_C) = (6.8$ ppm, -276 ppm) and (29.0 ppm, 172 ppm) for the CH and CH_3 groups, respectively. The signal intensity ratios of $[I(19\ \mu s)/I(4\ \mu s)]$ are 66 and 145% for the CH and CH_3 groups, respectively. The assignments based on the ratios are consistent with the assignments from the 1D data in Fig. 4, as discussed above. Thus, it is clear that we can obtain reliable assignment for ^{13}C and ^1H resonances for protonated carbons from a small number of 2D $^{13}C/^1H$ correlation NMR experiments with dipolar INEPT transfer.

For non-protonated $^{13}CO_2^-$, we identified two weaker cross-peaks at $(\omega_H, \omega_C) = (6.8$ ppm, -191 ppm) and (29.0 ppm, -191 ppm), which are marked by red solid and blue dotted squares in Fig. 5a. The peak at $(\omega_H, \omega_C) = (6.8$ ppm, -191 ppm) is assigned to a cross-peak between C^1H and $^{13}CO_2^-$ while the peak at (29.0 ppm, -191 ppm) is to a cross-peak between C^1H_3 and $^{13}CO_2^-$. We found that quantitative analysis of the cross-peak intensities provide structural information on medium-range ^{13}C–^1H distances. Fig. 5b shows τ-dependence of signal intensities for the cross-peaks from C^1H_3 (blue triangle) and C^1H (red square) to $^{13}CO_2^-$. The signal intensities were normalized to the maximum signal intensity for the cross-peak within the CH group ($\tau = 34$ μs). The cross-peak intensity was also divided by the number of the relevant protons so that the build-up rate of the cross-peak intensity can be easily correlated with the dipolar coupling constant between the relevant ^{13}C–^1H pair. Namely, we reduced the intensity of the cross-peak from C^1H_3 by a factor of 1/3. From Fig. 5b, it is clear that the cross-peak from C^1H to $^{13}CO_2^-$ shows faster polarization-transfer rate than that from C^1H_3. The τ-dependence curves obtained by numerical simulation show the best-fit results for the ^1H–^{13}C distances of 2.0 Å (red solid line) and 2.8 Å (blue dotted line) for the cross-peaks from CH and CH_3 protons, respectively. The obtained results agree well with the X-ray distances of 2.06 and 2.94 Å for CH and CH_3, respectively, where the latter is the average distance for three methyl protons [64]. This result clearly shows that medium-range ^{13}C–^1H distance information can be obtained by quantitative analysis of cross-peak intensities for a paramagnetic complex.

Fig. 6 shows a 2D $^{13}C/^1H$ correlation NMR spectrum of $Mn(acac)_3$ obtained using dipolar INEPT transfer with $\tau = 5$ μs (a) and 13 μs (b). In the experiment, we also used the pulse sequence in Fig. 2b. To enhance the sensitivity, the t_1 increment was set to one rotor period (36 μs) so that numerous sidebands in the ^1H dimension were folded into a central peak position. In the 2D spectrum, we could identify five strong signals except for sidebands for the system having ^{13}C paramagnetic shift dispersion over 1500 ppm. Using τ-dependence of signal intensity in the dipolar INEPT sequence, we assigned signals by comparing the signal intensities in Fig. 6a and b, as summarized in Table 1 in comparison with the assignment based on a separate 1D ^{13}C–^1H dipolar REDOR experiment. Most signals are well resolved by ^{13}C shifts. However, the two CH signals, which overlap in the 1D spectrum in Fig. 3f, are clearly resolved at $(\omega_H, \omega_C) = (5$ ppm, 350 ppm) and (9 ppm, 346 ppm), as indicated by the arrows in Fig. 6a. Assignments can be obtained by comparing the intensities of the signals at ^{13}C projections in Fig. 6a and b. It is apparent that the CH_3 signals increased and the CH signals slightly decreased as τ was increased. In the 2D spectra, we identified three CH_3 signals and two CH signals. The intensity ratios

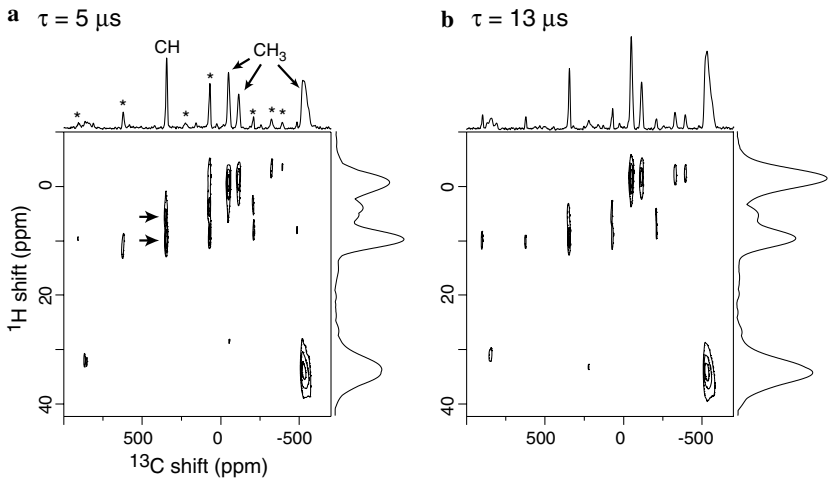

Fig. 6. 2D $^{13}C/^{1}H$ correlation NMR spectra of $Mn(acac)_3$ obtained with dipolar INEPT with $\tau = 5$ μs (a) and 13 μs (b) at −15 °C. The assignments were obtained by comparison of the signal intensities in the two data sets. For both of ^{1}H and ^{13}C spins, π/2- and π-pulse widths were 1.7 and 3.3 μs, respectively. The spinning speed was 27,778 ± 10 Hz. Thirty-six t_1 complex points were recorded with a t_1 increment of 36.0 μs (τ_R) and 174,080 scans for the real and imaginary components of each t_1 point. The recycle time was 2.8 ms including a signal acquisition period (0.8 ms) for each scan, and the total experimental time was 5 h each. Gaussian broadening of 800 Hz was applied in the t_1 and t_2 periods.

Table 1
Signal assignments for $Mn(acac)_3$ by 2D dipolar INEPT and 1D ^{13}C–^{1}H REDOR

^{13}C shift (ppm)[a]	517	350	348	−47	−113	−530
$I(13\ \mu s)/I(5\ \mu s)$ (%)[b]	—[e]	81 ± 5	77 ± 7	154 ± 8	136 ± 11	160 ± 5
Assignment by dipolar INEPT	—	CH	CH	CH_3	CH_3	CH_3
S/S_0 (%) in ^{13}C–^{1}H REDOR[c]	88 ± 3	24 ± 1		61 ± 1	64 ± 2	52 ± 1
Assignment by ^{13}C–^{1}H REDOR[d]	CO	CH		CH_3	CH_3	CH_3

[a] Chemical shifts were adopted from the 2D $^{13}C/^{1}H$ correlation spectrum in Fig. 6a. The values are slightly different from those in 1D spectrum in Fig. 3 because of the temperature dependence of paramagnetic shifts.

[b] The signals satisfying $50\% \leqslant I(13\ \mu s)/I(5\ \mu s) \leqslant 90\%$ and $100\% \leqslant I(13\ \mu s)/I(5\ \mu s) < 180\%$ were assigned to CH and CH_3, respectively. In a control experiment for L-Ala using the same conditions, we obtained $I(13\ \mu s)/I(5\ \mu s) = 71\%$, 128% for ^{13}CH, $^{13}CH_3$ groups.

[c] S and S_0 denote signal intensities with and without ^{1}H π-pulses, which introduce dephasing due to ^{13}C–^{1}H dipolar couplings. The experiments were performed at spinning speed of 28,571 Hz at −15 °C. ^{1}H and ^{13}C RF intensities were 250 and 150 kHz, respectively. See Ref. [42] about other experimental details.

[d] The signals satisfying $S/S_0 \leqslant 25\%$, $25\% \leqslant S/S_0 \leqslant 65\%$, $75\% \leqslant S/S_0$ were assigned to CH, CH_3, and CO, respectively. In a control experiment on L-Val using the same conditions, we obtained $S/S_0 = 5$, 45, 85% for ^{13}CH, $^{13}CH_3$, and $^{13}CO_2^-$ groups.

[e] Not analyzed for this resonance.

$I(13\ \mu s)/I(5\ \mu s)$ for the CH and CH_3 groups are 77–81% and 136–160%, respectively. These values reasonably agree with 71% and 128% obtained for CH and CH_3 of L-Ala, respectively. The sidebands due to paramagnetic dipolar shifts observed for CH_3 groups are fewer; this is consistent with the X-ray structures, in which the CH_3 groups are more remotely located from Mn(III) ($R_{C-Mn} = 4.4$ Å) than CO (3.0 Å) or CH (3.3 Å) groups [65]. The two CH signals at $(\omega_H, \omega_C) = (5\ ppm, 350\ ppm)$ and $(9\ ppm, 346\ ppm)$ have an intensity ratio 1:2; hence it is likely that signals for two CH groups are overlapping at (9 ppm, 346 ppm). The ratio of integral intensities for the CH_3 signals at $(\omega_H, \omega_C) = (34\ ppm, -530\ ppm)$, $(-2\ ppm, -47\ ppm)$, and $(-2\ ppm, -113\ ppm)$ is 3.3:1.8:1.0, which is approximately 3:2:1. Hence, we consider that three and two CH_3 signals are overlapping at the former two positions. These results suggest that the existence of three non-equivalent ligand molecules in $Mn(acac)_3$, which is consistent with recent X-ray crystallography results [65]. In the present spectra, the cross-peak for ^{13}CO at 517 ppm was too weak to be properly analyzed. In addition to the five strong peaks, we also identified weak cross-peaks at $(\omega_H, \omega_C) = (32\ ppm, 840\ ppm)$, which may be assigned to another ^{13}CO group. Although distance measurements were difficult for this sample, the present result shows that 2D $^{13}C/^{1}H$ correlation NMR is possible for the paramagnetic system with more than 1000 ppm spectral dispersion, providing high-resolution and reliable assignment for ^{1}H and ^{13}C SSNMR.

4. Conclusion

The strategies presented here provide a simple solution for characterization and structural studies by ^{13}C SSNMR for a variety of paramagnetic systems, which had been difficult to analyze by existing SSNMR methods. Our results

showed that useful information such as ^{13}C–^{1}H distances, existence of non-equivalent sites, and distortion from the symmetry can be detected for small amount of paramagnetic complexes. As shown recently by Oldfield et al., with reliable signal assignment, experimental isotropic paramagnetic shifts can be combined with ab initio calculations to elucidate structures of paramagnetic systems [64]. We believe that the VFMAS approach presented here is useful for molecular-level characterization of paramagnetic systems, including drugs, biomimetics, and advanced materials.

In this study, we only focused on ^{13}C SSNMR for small unlabeled paramagnetic systems. However, it is obvious that similar strategies are applicable to other spin-1/2 nuclei such as ^{15}N, ^{29}Si, ^{31}P in paramagnetic materials. Polenova et al. showed that 1D SSNMR of abundant ^{31}P spins can be obtained for an interesting inorganic paramagnetic system, polyoxometalate [66]. Our methods presented here should be applicable to such systems to correlate ^{31}P resonances with ^{1}H or other dilute spin-1/2 nuclei. The excellent sensitivity and resolution obtained in this study also suggests the possibility of analyzing ^{13}C-labeled paramagnetic systems with higher molecular weights, such as metal–peptide/protein complexes, by SSNMR. Jovanovic and McDermott recently examined SSNMR of selectively ^{13}C- and ^{15}N-labeled P450 BM-3 heme protein; they observed well-resolved 2D SSNMR spectra for selectively labeled ^{13}C and ^{15}N sites that are remotely located ($\sim$9 Å) from the paramagnetic metal center with assignments [67]. Although these resonances were subject to only slight paramagnetic shifts, with our VFMAS approach, it may be possible to observe $^{13}C/^{15}N$ sites in the vicinity of metal centers in the presence of large paramagnetic shifts.

Acknowledgments

We are grateful to Professor Cynthia Jameson at UIC for her kind suggestions and stimulating discussions. This study was supported in part by grants from Alzheimer's Association (NIRG 035123) and the NSF CAREER program (CHE 449952).

References

[1] I. Bertini, H.B. Gray, S.J. Lippard, J.S. Valentine, Bioinorganic Chemistry, University Science Books, Sausalito, CA, 1994.
[2] J.M. Lehn, Supramolecular Chemistry: Concepts and Perspectives, VCH-Weinheim, New York, 1995.
[3] J.L. Atwood, J.E. Davis, D.D. MacNicol, F. Vogtle, Comprehensive Supramolecular Chemistry, Elsevier Science, Oxford, 1996.
[4] M.J. Abrams, B.A. Murrer, Metal-compounds in therapy and diagnosis, Science 261 (1993) 725–730.
[5] N.P. Farrell, Uses of Inorganic Chemistry in Medicine, Royal Society of Chemistry, Cambridge, 1999.
[6] K.H. Thompson, C. Orvig, Boon and bane of metal ions in medicine, Science 300 (2003) 936–939.
[7] T. Tanaka, F. Toda, Solvent-free organic synthesis, Chem. Rev. 100 (2000) 1025–1074.
[8] M. Mehring, High Resolution NMR in Solids, Springer-Verlag, New York, 1983.
[9] S.J. Opella, F.M. Marassi, Structure determination of membrane proteins by NMR spectroscopy, Chem. Rev. 104 (2004) 3587–3606.
[10] K. Schmidt-Rohr, H.W. Spiess, Multidimensional Solid-state NMR and Polymers, Academic Press, San Diego, 1994.
[11] R.G. Griffin, Dipolar recoupling in MAS spectra of biological solids, Nat. Struct. Biol. 5 (1998) 508–512.
[12] M.J. Duer (Ed.), Solid-state NMR Spectroscopy Principles and Applications, Blackwell Science, Oxford, 2002.
[13] A.E. McDermott, Structural and dynamic studies of proteins by solid-state NMR spectroscopy: rapid movement forward, Curr. Opin. Struct. Biol. 14 (2004) 554–561.
[14] D. McElheny, E. DeVita, L. Frydman, Heteronuclear local field NMR spectroscopy under fast magic-angle sample spinning conditions, J. Magn. Reson. 143 (2000) 321–328.
[15] Y. Ishii, ^{13}C–^{13}C dipolar recoupling under very fast magic angle spinning in solid-state NMR: applications to distance measurements, spectral assignments, and high-throughput secondary-structure elucidation, J. Chem. Phys. 114 (2001) 8473–8483.
[16] K. Schmidt-Rohr, J.-D. Mao, Efficient CH-group selection and identification in 13C solid-state NMR by dipolar DEPT and 1H chemical-shift filtering, J. Am. Chem. Soc. 124 (2002) 13938–13948.
[17] K.A.H. Wildman, D.K. Lee, A. Ramamoorthy, Determination of alpha-helix and beta-sheet stability in the solid state: a solid-state NMR investigation of poly(L-alanine), Biopolymers 64 (2002) 246–254.
[18] M. Wind, K. Saalwachter, U.M. Wiesler, K. Mullen, H.W. Spiess, Solid-state NMR investigations of molecular dynamics in polyphenylene dendrimers: evidence of dense-shell packing, Macromolecules 35 (2002) 10071–10086.
[19] E.K. Paulson, C.R. Morcombe, V. Gaponenko, B. Dancheck, R.A. Byrd, K.W. Zilm, High-sensitivity observation of dipolar exchange and NOEs between exchangeable protons in proteins by 3D solid-state NMR spectroscopy, J. Am. Chem. Soc. 125 (2003) 14222–14223.
[20] D. Marulanda, M.L. Tasayco, A. McDermott, M. Cataldi, V. Arriaran, T. Polenova, Magic angle spinning solid-state NMR spectroscopy for structural studies of protein interfaces. Resonance assignments of differentially enriched *Escherichia coli* thioredoxin reassembled by fragment complementation, J. Am. Chem. Soc. 126 (2004) 16608–16620.
[21] A.T. Petkova, R.D. Leapman, Z.H. Guo, W.M. Yau, M.P. Mattson, R. Tycko, Self-propagating, molecular-level polymorphism in Alzheimer's beta-amyloid fibrils, Science 307 (2005) 262–265.
[22] K.T. Mueller, B.Q. Sun, G.C. Chingas, J.W. Zwanziger, T. Terao, A. Pines, Dynamic-Angle Spinning of quadrupolar nuclei, J. Magn. Reson. 86 (1990) 470–487.
[23] L. Frydman, J.S. Harwood, Isotropic spectra of half-integer quadrupolar spins from bidimensional magic-angle-spinning nmr, J. Am. Chem. Soc. 117 (1995) 5367–5368.
[24] Z.H. Gan, Satellite transition magic-angle spinning nuclear magnetic resonance spectroscopy of half-integer quadrupolar nuclei, J. Chem. Phys. 114 (2001) 10845–10853.
[25] C.P. Grey, A.J. Vega, Determination of the quadrupole coupling-constant of the invisible aluminum spins in zeolite Hy with H-1/Al-27 trapdor nmr, J. Am. Chem. Soc. 117 (1995) 8232–8242.
[26] T. Gullion, Measurement of dipolar interactions between spin-1/2 and quadrupolar nuclei by rotational-echo, adiabatic-passage, double-resonance NMR, Chem. Phys. Lett. 246 (1995) 325–330.
[27] E. Hughes, J. Jordan, T. Gullion, Structural characterization of the Cs(*p-tert*-butylcalix 4 arene -H)(MeCN) guest–host system by C-13-Cs-133 REDOR NMR, J. Phys. Chem. B 105 (2001) 5887–5891.
[28] T. Gullion, A.J. Vega, Measuring heteronuclear dipolar couplings for $I = 1/2$, $S > 1/2$ spin pairs by REDOR and REAPDOR NMR, Prog. Nucl. Magn. Reson. Spectrosc. 47 (2005) 123–136.
[29] L. van Wullen, H-1-C-13-Al-27 triple resonance transfer of populations in double resonance experiments for the detection of C-13-Al-27 dipolar interactions, Solid State Nucl. Magn. Reson. 13 (1998) 123–127.

[30] V.P. Chacko, S. Ganapathy, R.G. Bryant, 13C CP-MAS NMR spectra of paramagnetic solids, J. Am. Chem. Soc. 105 (1983) 5491–5492.
[31] T.H. Walter, E. Oldfield, Magic-angle sample-spinning N. M. R. spectroscopy of an antiferromagnetically coupled copper formate dimer, J. Chem. Soc., Chem. Commun. (1987) 646–647.
[32] C.P. Grey, C.M. Dobson, A.K. Cheetham, R.J. Jakeman, Studies of rare-earth stannates by 119Sn MAS NMR. The use of paramagnetic shift probes in solid state, J. Am. Chem. Soc. 111 (1989) 505–511.
[33] A.N. Clayton, C.M. Dobson, C.P. Grey, High resolution 13C MAS NMR spectra of paramagnetic lanthanide complexes, J. Chem. Soc., Chem. Commun. (1990) 72–74.
[34] K. Liu, D. Ryan, K. Nakanishi, A. McDermott, Solid-state NMR-studies of paramagnetic coordination-complexes—a comparison of protons and deuterons in detection and decoupling, J. Am. Chem. Soc. 117 (1995) 6897–6906.
[35] T.P. Spaniol, A. Kubo, T. Terao, Resolution enhancement of magic angle spinning NMR spectra for paramagnetic zero-quantum NMR, Mol. Phys. 96 (1999) 827–834.
[36] G.C. Campbell, J.F. Haw, Determination of magnetic and structural properties in solids containing antiferromagnetically coupled metal centers using NMR methods. Magneto-structural correlations in anhydrous copper(II) *n*-butyrate, Inorg. Chem. 27 (1988) 3706–3709.
[37] M. Crozet, M. Chaussade, M. Bardet, L. Emsley, B. Lamotte, J.M. Mouesca, Carbon-13 solid-state NMR studies on synthetic model compounds of 4Fe–4S clusters in the 2(+) state, J. Phys. Chem. A 104 (2000) 9990–10000.
[38] H. Heise, F.H. Kohler, X.L. Xie, Solid-state NMR spectroscopy of paramagnetic metallocenes, J. Magn. Reson. 150 (2001) 198–206.
[39] S. Aime, I. Beritini, C. Luchinat, Considerations on high resolution solid state NMR in paramagnetic molecules, Coord. Chem. Rev. 150 (1996) 221–242.
[40] A. Nayeem, J.P. Yesinowski, Calculation of magic-angle spinning nuclear magnetic resonance spectra of paramagnetic solids, J. Chem. Phys. 89 (1988) 4600–4608.
[41] A.R. Brough, C.P. Grey, C.M. Dobson, Paramagnetic ions as structural probes in solid-state NMR: distance measurements in crystalline lanthanide acetates, J. Am. Chem. Soc. 115 (1993) 7318–7327.
[42] Y. Ishii, S. Chimon, N.P. Wickramasinghe, A new approach in 1D and 2D 13C high resolution solid-state NMR spectroscopy of paramagnetic organometallic complexes by very fast magic-angle spinning, J. Am. Chem. Soc. 125 (2003) 3438–3439.
[43] M. Baldus, D.G. Geurts, B.H. Meier, Broadband dipolar recoupling in rotating solids: a numerical comparison of some pulse schemes, Solid State Nucl. Magn. Reson. 11 (1998) 157–168.
[44] N.P. Wickramasinghe, M. Shaibat, Y. Ishii, Enhanced sensitivity and resolution in 1H solid-state NMR spectroscopy of paramagnetic complexes under very fast magic angle spinning, J. Am. Chem. Soc. 127 (2005) 5796–5797.
[45] M. Ernst, A. Samoson, B.H. Meier, Low-power XiX decoupling in MAS NMR experiments, J. Magn. Reson. 163 (2003) 332–339.
[46] E.D. Vita, L. Frydman, Spectral editing in13C MAS NMR under moderately fast spinning conditions, J. Magn. Reson. 148 (2001) 327–337.
[47] F. Delaglio, S. Grzesiek, G.W. Vuister, G. Zhu, J. Pfeifer, A. Bax, Nmrpipe—a multidimensional spectral processing system based on Unix pipes, J. Biomol. NMR 6 (1995) 277–293.
[48] S. Hediger, B.H. Meier, R.R. Ernst, Adiabatic passage Hartmann–Hahn cross polarization in NMR under magic angle sample spinning, Chem. Phys. Lett. 240 (1995) 449–456.
[49] A.C. Kolbert, A. Bielecki, Broadband Hartmann–Hahn matching in magic-angle spinning NMR via an adiabatic frequency sweep, J. Magn. Reson. A 116 (1995) 29–35.
[50] K. Saalwachter, R. Graf, H.W. Spiess, Recoupled polarization-transfer methods for solid-state H-1-C-13 heteronuclear correlation in the limit of fast MAS, J. Magn. Reson. 148 (2001) 398–418.
[51] B. Bleaney, Nuclear magnetic resonance shifts in solution due to lanthanide ions, J. Magn. Reson. 8 (1972) 91–100.
[52] T. Mildner, H. Ernst, D. Freude, Pb-207 nmr detection of spinning-induced temperature-gradients in mas rotors, Solid State Nucl. Magn. Reson. 5 (1995) 269–271.
[53] I. Bertini, C. Luchinat, G. Parigi, Solution NMR of Paramagnetic Molecules, Elsevier Science B.V., Amsterdam, The Netherlands, 2001.
[54] R.R. Ernst, G. Bodenhausen, A. Wokaun, Principles of Nuclear Magnetic Resonance in One and Two Dimensions, Oxford University Press, Oxford, 1987.
[55] J. Krzystek, G.J. Yeagle, J.H. Park, R.D. Britt, M.W. Meisel, L.C. Brunel, J. Telser, High-frequency and -field EPR spectroscopy of *tris*(2,4-pentanedionato)manganese(III): investigation of solid-state versus solution Jahn–Teller effects, Inorg. Chem. 42 (2003) 4610–4618.
[56] J. Herzfeld, A.E. Berger, Sideband intensities in NMR spectra of samples spinning at the magic angle, J. Chem. Phys. 73 (1980) 6021–6030.
[57] X.L. Wu, S.T. Burns, K.W. Zilm, Spectral editing in cpmas nmr—generating subspectra based on proton multiplicities, J. Magn. Reson. A 111 (1994) 29–36.
[58] S.T. Burns, X.L. Wu, K.W. Zilm, Improvement of spectral editing in solids: a sequence for obtaining (CH)-C-13 + (CH2)-C-13-only C-13 spectra, J. Magn. Reson. 143 (2000) 352–359.
[59] R. Calvo, P.R. Levstein, E.E. Castellano, S.M. Fabiane, O.E. Piro, S.B. Oseroff, Crystal-structure and magnetic-interactions in bis(D,L-alaninato)copper(II) hydrate, Inorg. Chem. 30 (1991) 216–220.
[60] X.L. Yao, K. Schmidt-Rohr, M. Hong, Medium- and long-distance H-1-C-13 heteronuclear correlation NMR in solids, J. Magn. Reson. 149 (2001) 139–143.
[61] Alia, J. Matysik, I. de Boer, P. Gast, H.J. van Gorkom, H.J.M. de Groot, Heteronuclear 2D (H-1-C-13) MAS NMR resolves the electronic structure of coordinated histidines in light-harvesting complex II: Assessment of charge transfer and electronic delocalization effect, J. Biomol. NMR 28 (2004) 157–164.
[62] X.L. Yao, V.P. Conticello, M. Hong, Investigation of the dynamics of an elastin-mimetic polypeptide using solid-state NMR, Magn. Reson. Chem. 42 (2004) 267–275.
[63] B. Elena, A. Lesage, S. Steuernagel, A. Bockmann, L. Emsley, Proton to carbon-13 INEPT in solid-state NMR spectroscopy, J. Am. Chem. Soc. 127 (2005) 17296–17302.
[64] Y. Zhang, H.H. Sun, E. Oldfield, Solid-state NMR Fermi contact and dipolar shifts in organometallic complexes and metalloporphyrins, J. Am. Chem. Soc. 127 (2005) 3652–3653.
[65] B.R. Stults, R.S. Marianelli, V.W. Day, Distortions of the coordination polyhedron in high-spin manganese(III) complexes. 3. Crystal and molecular structure of .gamma.-*tris*(acetylacetonato)manganese(III): a tetragonally elongated octahedral form, Inorg. Chem. 18 (1979) 1853–1858.
[66] X.M. Zhang, C. Zhang, H.Q. Guo, W.L. Huang, T. Polenova, L.C. Francesconi, D.L. Akins, Optical spectra of a novel polyoxometalate occluded within modified MCM-41, J. Phys. Chem. B 109 (2005) 19156–19160.
[67] T. Jovanovic, A.E. McDermott, Observation of ligand binding to cytochrome P450-BM-3 by means of solid-state NMR spectroscopy, J. Am. Chem. Soc. 127 (2005) 13816–13821.